Computation of EM Fields Inside A Spheroidal Head Due To A Thin Circular-Loop: A Higher-Order Perturbation Approach

Mui-Seng Yeo
National University of Singapore
Department of Electrical Engineering

Abstract

This paper presents an alternative analysis of obtaining radiated EM fields on a human head, using Perturbation technique. A circular-loop antenna is use as a radiator, and the head is modeled by a spheroid. This method make use of dyadic Green's function to obtain the incident EM field. The spheroid is approximated using Taylor series expansion, and coefficients for transmission and scattering EM field are found using the perturbation method. These coefficients are also being expanded into Taylor series like terms, and with the boundary conditions on the spheroid surface, the coefficients can be found.

I. Introduction

THE harzard radiation on human body by EM waves energy have been of interest in many research areas, [1], [2], [3] and [4]. Apart from harmful effects, EM radiation have been use for therapeutic purposes in cancer tumor treatment, [5]. Thus, it is necessarily to determine the deposition of EM energy into the human body.

In the research area of EM waves, numerical methods have been widely used. Such works can be seen in papers by Lazzi and Gandhi [6], Jensen and Rahmat-Samii [7]. One of the advantages is that objects can be modeled with high accuracy. However, such methods require lot of computation time and storage space.

Another popluar way of obtaining EM radiation is by using analytical approach. The main advantage of using analytical solution can be computed faster and uses less storage. An example of such work is the paper by Uzunoglu and Angelikas, [5].

Recently, the paper by Li *et al*, [8], demonstrated the rigorous formulation of EM fields within a spherical multilayered media. Dyadic Green's function was use, and the current sources are arbitrary, such that they can be located in one of the layers.

II. Formulation of The Problem

Consider the geometry in Fig. 1, where the origin is located in the center of the spheroid. The circular antenna is located directly above spheroid in the z-direction. Many works had been done in deriving the EM waves by circular antenna, and some of them are found in [9], [10], [11] and [12].

Assume that the current in the antenna is $I(\phi')$, the volumetric current density can be expressed as :

$$\boldsymbol{J}(\boldsymbol{r}') = \frac{I(\phi')\delta(r'-\rho_0)\delta(\theta'-\theta_0)}{r_0^2\sin\theta'}\widehat{\boldsymbol{\phi}} \tag{1}$$

where $\rho_0 = \frac{r_0}{\sin\theta}$.

In spherical coordinates, the equation of spheroid can be written as, [13] $r = \frac{h}{\sqrt{1-\nu\sin^2\theta}}$ where $\nu = 1-\left(\frac{h}{w}\right)^2$, and $\frac{h}{w} > 1$. The unit normal vector on the surface can be written as $\widehat{\boldsymbol{n}} = n_r\widehat{\boldsymbol{r}} + n_\theta\widehat{\boldsymbol{\theta}}$.

The equation for the E-field is given as [14] :

$$\boldsymbol{E} = i\omega\mu_0 \iiint_V \overline{\boldsymbol{G}}_{EJ0}(\boldsymbol{r},\boldsymbol{r}')\cdot\boldsymbol{J}(\boldsymbol{r}')dV' \tag{2}$$

Substituting (1) into (2), the E-field can be written as :

$$\left[\begin{array}{c} \boldsymbol{E}^{>} \\ \boldsymbol{E}^{<} \end{array}\right] = \frac{-\eta_0 k_0^2}{4\pi} \sum_{n=1}^{\infty} \sum_{m=0}^{n} (2-\delta_{m0}) D_{mn} \left\{ \left[\begin{array}{c} \Phi_{\substack{e_{mn} \\ o_{mn}}}^{M<} \boldsymbol{M}_{\substack{e_{mn} \\ o_{mn}}}^{(1)}(k_0) \\ \Phi_{\substack{e_{mn} \\ o_{mn}}}^{M>} \boldsymbol{M}_{\substack{e_{mn} \\ o_{mn}}}(k_0) \end{array}\right] + \left[\begin{array}{c} \Phi_{\substack{e_{mn} \\ o_{mn}}}^{N<} \boldsymbol{N}_{\substack{e_{mn} \\ o_{mn}}}^{(1)}(k_0) \\ \Phi_{\substack{e_{mn} \\ o_{mn}}}^{N>} \boldsymbol{N}_{\substack{e_{mn} \\ o_{mn}}}(k_0) \end{array}\right] \right\} \tag{3}$$

where $>$ and $<$ attached to $\boldsymbol{E}$ refers to E-field when $r > \rho_0$ and $r < \rho_0$ respectively. δ_{m0} and D_{mn} are defined in [9]. The coefficients $\Phi_{\substack{e_{mn} \\ o_{mn}}}^{M<}(k)$, $\Phi_{\substack{e_{mn} \\ o_{mn}}}^{M>}(k)$, $\Phi_{\substack{e_{mn} \\ o_{mn}}}^{N<}(k)$ and $\Phi_{\substack{e_{mn} \\ o_{mn}}}^{N<}(k)$ are given by :

$$\left[\begin{array}{c} \Phi_{\substack{e_{mn} \\ o_{mn}}}^{M<} \\ \Phi_{\substack{e_{mn} \\ o_{mn}}}^{M>} \end{array}\right] = -\frac{r_0}{\sin\theta_0} \left[\begin{array}{c} j_n(k_0\rho_0) \\ h_n^{(1)}(k_0\rho_0) \end{array}\right] \frac{dP_n^m(\cos\theta_0)}{d\theta}\bigg|_{\theta=\theta_0} \int_0^{2\pi} \begin{array}{c} \cos \\ \sin \end{array} (m\phi') I(\phi') d\phi', \tag{4}$$

$$\left[\begin{array}{c} \Phi_{\substack{e_{mn} \\ o_{mn}}}^{N<} \\ \Phi_{\substack{e_{mn} \\ o_{mn}}}^{N>} \end{array}\right] = \mp\frac{r_0}{\sin\theta_0} \left[\begin{array}{c} \frac{d[rj_n(k_0r)]}{k_0 r dr}\Big|_{r=\rho_0} \\ \frac{d[rh_n^{(1)}(k_0r)]}{k_0 r dr}\Big|_{r=\rho_0} \end{array}\right] m P_n^m(\theta_0) \int_0^{2\pi} \begin{array}{c} \sin \\ \cos \end{array} (m\phi') I(\phi') d\phi'. \tag{5}$$

.

The magnetic field can be obtained by using $\boldsymbol{H} = \frac{1}{j\omega\mu_0} \nabla \times \boldsymbol{E}$.

(3) is the E-field radiated by the antenna in the free space and they will be denoted by $\boldsymbol{H}_i$ and $\boldsymbol{E}_i$. The transmitted fields in the spheroid can be written as :

$$\left[\begin{array}{c} \boldsymbol{E}_t^{>} \\ \boldsymbol{E}_t^{<} \end{array}\right] = \frac{-\eta_0 k_1^2}{4\pi} \sum_{n=1}^{\infty} \sum_{m=0}^{n} (2-\delta_{m0}) D_{mn} \left\{ \alpha \left[\begin{array}{c} \Phi_{\substack{e_{mn} \\ o_{mn}}}^{M<} \boldsymbol{M}_{\substack{e_{mn} \\ o_{mn}}}^{(1)}(k_1) \\ \Phi_{\substack{e_{mn} \\ o_{mn}}}^{M>} \boldsymbol{M}_{\substack{e_{mn} \\ o_{mn}}}(k_1) \end{array}\right] + \zeta \left[\begin{array}{c} \Phi_{\substack{e_{mn} \\ o_{mn}}}^{N<} \boldsymbol{N}_{\substack{e_{mn} \\ o_{mn}}}^{(1)}(k_1) \\ \Phi_{\substack{e_{mn} \\ o_{mn}}}^{N>} \boldsymbol{N}_{\substack{e_{mn} \\ o_{mn}}}(k_1) \end{array}\right] \right\} \tag{6}$$

where $k_1 = \sqrt{\epsilon_r} k_0$, ϵ_r is the relative permittivity of the spheroid. The constants α and ζ are unknown transmission coefficients. For scattered field $\boldsymbol{E}_s$, α and ζ in (6) are placed by scattering coefficients β and γ respectively.

For a small loop antenna, the current distribution will be approximately constant : $\boldsymbol{I}(\phi') = I_0 \widehat{\boldsymbol{\phi}}$.

Applying the small antenna model, the boundary conditions can be written as :

$$\widehat{\boldsymbol{n}} \times \boldsymbol{E}_i = \widehat{\boldsymbol{n}} \times (\boldsymbol{E}_s + \boldsymbol{E}_t) \tag{7}$$

$$\widehat{\boldsymbol{n}} \times \boldsymbol{H}_i = \widehat{\boldsymbol{n}} \times (\boldsymbol{H}_s + \boldsymbol{H}_t) \tag{8}$$

III. Determination of Expansion coefficients

A. Perturbation Technique

Perturbation approximation can be use to solve for the coefficients, which is demonstrated in [15]. Perturbating terms can be added, and each higher order terms must converge. The parameters and unknown coefficients are expanded using Taylor series. By solving (7) and (8), the first 4 orders of coefficients were obtained.

IV. Numerical Computation

The numerical parameters that are use in the computation are : Relative permittivity $\epsilon_r = 42$, frequency $f = 5$ MHz, antenna radius $r = 0.25$m, and antenna position $\theta_0 = \frac{\pi}{3}$ rad.

A. Tranmission and Scattering Coefficients with varying ν

Setting $h = 0.1$m and $w = 0.06$m, $\nu = -1.78$. Since $|\nu| > 1$, the coefficients computed fails to converge. Setting $w = 0.08$m, $|\nu| = 0.56$, Table I shows the numerical coefficients terms computed.

The number of orders to be use for computing E-fields will depends on the aspect ratio of the spheroid. For a large ratio, more higher order terms will be needed to achieve a respectable accuracy. If the ratio is too large, where $|\nu|$ is larger than 1, perturbation method will fail as the coefficients and E-fields will fail to converge.

B. Tranmission and Scattering Coefficients with varying frequency

By varying the frequency at which the antenna operates at from 0.5MHz to 500MHz, the convergence of β and α are checked. Calculations are based on $|\nu| = 0.56$. At frequency 0.5MHz, $k_0 r_0 = 2.62 \times 10^{-3}$. The coefficients converge rapidly with increasing order. At frequency 5MHz, $k_0 r_0 = 2.62 \times 10^{-2}$. The values of the coefficients are as shown in Table I. At this frequency, the convergence is slower than 0.5MHz. When the frequency is further increased to 500MHz, $k_0 r_0 = 2.62$, the antenna can no longer considered small, and thus, the current distribution in the antenna varies with ϕ and convergence fails.

TABLE I
β AND α FOR THE FIRST 10 VALUES OF n FOR $\nu = 0.56$

	β, Orders				α, Orders, $A(B) \equiv A \times 10^B$			
n	0^{th}	1^{st}	2^{nd}	3^{rd}	0^{th}	1^{st}	2^{nd}	3^{rd}
1	0.512	0.017	0.0090	0.0053	1.20(−6)	1.37(−6)	1.17(−6)	9.64(−6)
2	0.536	0.008	0.0031	0.0016	3.68(−9)	4.25(−9)	3.67(−9)	2.93(−9)
3	0.670	0.222	0.0890	0.0308	6.36(−13)	2.94(−11)	5.06(−11)	5.97(−11)
4	0.769	0.056	0.0184	0.0090	7.03(−17)	1.12(−15)	1.86(−15)	2.14(−15)
5	0.822	0.011	0.0034	0.0292	5.38(−21)	2.37(−20)	3.44(−19)	8.18(−19)
6	0.854	0.075	0.0232	0.0099	3.03(−25)	1.15(−23)	1.30(−22)	2.70(−22)
7	0.876	0.031	0.0096	0.0945	1.30(−29)	2.61(−28)	9.49(−28)	5.46(−27)
8	0.893	0.007	0.0025	0.0273	4.43(−34)	2.75(−33)	2.80(−32)	2.97(−31)
9	0.905	0.044	0.0128	0.0747	1.21(−38)	5.35(−37)	7.32(−36)	2.49(−35)
10	0.915	0.021	0.0065	0.0154	2.77(−43)	6.98(−42)	3.36(−41)	1.05(−40)

C. Convergence of E-fields

The convergence of E-fields as the order increases is investigated. The parameter of the spheroid is set to $h = 0.1$m, $w = 0.08$m, and $|\nu| = 0.56$. The transmitted field in the spheroid is computed at $r = 0.05$m, and $\theta = \frac{\pi}{4}$ rad. At $n = 10$, the E-field is about 7 orders smaller than $n = 1$, which implies that the contribution at $n > 10$ can be ignored. For scattered field computed at $r = 0.102$m, at $n = 10$, it is almost 7 orders smaller than at $n = 1$. Therefore, it is only necessarily to compute for the first 10 n terms only.

D. Approximations for Higher Order of E-fields

From Fig.2, the converging pattern allows for a graphical approximation of higher order of E-fields. It appears that E-field at different orders are bounded by 2 converging exponential curves. For odd orders (first and third), the E-fields falls on a lower boundary curve, while even orders' E-fields fall on a upper boundary curve. By using this approximation, higher order of E-field can be predicted.

E. SAR with varying antenna position

The SAR in the spheroid is calculated using the equation (as used in [5]) : $SAR = \frac{\sigma|\boldsymbol{E}|^2}{2\rho}$ where the conductivity and density of spheroid are assumed to be constant at $\sigma = 0.65$S/m and $\rho = 1000$ kg/m^3 respectively. Table II shows the maximum SAR absorption on the surface of the spheroid at different antenna positions. From $\theta_0 = \frac{\pi}{6}$ to $\theta_0 = \frac{\pi}{2}$ rad, the SAR increases by a factor of almost 30.8 dB. Fig. **??** show the SAR distribution within the spheroid. The distributions are plotted for half, quarter, one-eight and one-sixteenth power. The maximum power being absorb tends in the direction of the antenna location. The heating pattern agrees with the results obtained in [5].

V. Conclusion

From the discussion above, perturbation techniques generally achieve the objective of predicting the EM fields and enable fast computation to obtain the result. However, there are some limitations due to the assumptions made.

Variations to the same problem can be made so that the model can be more realistic and accurate. Such variations includes having different current distribution in the antenna, different form of antenna and multi-layered spheroid.

References

[1] G Rauch, S Sussman, and N G Hingorani, "Electric and magnetic fields : Background on health effects and an update on epri research", *Electric Power Research Institute, USA*, pp. 200–204, -.

[2] Stephan P. Albert Bren, "Reviewing the RF safety issue in cellular telephones", *IEEE Engineering in Medicine and Biology*, pp. 109–115, May/June 1996.

[3] W.W. Shelton and J.C. Toler, "Bioeffects issues of power frequency magnetic fields", *IEEE*, 1993.

[4] R.E Johnson, "The new IEEE standard for exposures to RF/microwave energy and the instrumentation available to perform complicane measurements", *The Institution of Electrical engineers*, 1993.

[5] N.K. Uzunoglu and E.A. Angelikas, "Field distributions in a three-layer prolate spheroidal human body model for a loop antenna irradiation", *IEEE Trans. Antennas and Propagat.*, vol. AP-35, no. -, pp. 1180–1185, October 1987.

[6] Gianluca Lazzi and Om P. Gandhi, "On modeling and personal dosimetry of cellular telephone helical antennas with FDTD code", *IEEE Transactions on Antennas and Propagation*, vol. 46, no. 4, pp. 525–530, April, 1998.
[7] Michael A. Jensen and Yahaya Rahmat-Samii, "EM interaction o handset antennas and a human in personal communications", *Proceedings of IEEE*, vol. 83, no. 1, pp. 7–17, Jan., 1995.
[8] Le-Wei Li, Mook-Seng Leong, Pang-Shyan Kooi, and Tat-Soon Yeo, "Electromagnetic dyadic Green's function in in spherically multilayered media", *IEEE Trans. Antennas and Propagat.*, vol. 42, no. 12, pp. 2302–2310, Dec 1994.
[9] Le-Wei Li, Mook-Seng Leong, Pang-Shyan Kooi, and Tat-Soon Yeo, "Exact solutions of electromagnetic fields in both near and far zones radiated by thin circular-loop antennas : A general representation", *IEEE Trans. Antennas and Propagat.*, vol. 43, no. -, pp. 811–822, December 1997.
[10] Douglas H. Werner, "An exact integration procedure for vector potentials of thin circular loop antennas", *IEEE Trans. on Antennas and Propagat.*, vol. 44, no. 2, pp. 157–165, February 1996.
[11] P.L. Overfelt, "Near fields of the constant current thin circular loop antenna of arbitrary radius", *IEEE Trans. on Antennas and Propagat.*, vol. 44, no. 2, pp. 166–171, August 1978.
[12] Constantine A. Balanis, *Antenna Theory : Analysis and Design*, John Wiley and Sons, 1997.
[13] L.W. Li, P.S. Kooi, M.S. Leong, and T.S. Yeo, "Integral equation approximation to microwave scattering by distorted raindrops: The spheroidal model", in *Proc. of IEEE Singapore International Conference on Networks/Information Engineering* (SICON/ICIE'95), Shangri-La Hotel, Singapore, July 3-7, 1995, pp. 658–662.
[14] C.T. Tai, *Dyadic Green's Fuunctions in electromagnetic Theory*, 2nd ed. Piscataway, NI: IEEE Press, 1994.
[15] L.W. Li, P.S. Kooi, M.S. Leong, T.S. Yeo, and M.Z. Gao, "Microwave attenuation by realistically distorted raindrops: Part I–Theory", *IEEE Trans. Antennas Propagat.*, vol. 43, no. 8, pp. 811–822, August 1995.

TABLE II

SAR distributions at different antenna's position

θ_0, rad	$\frac{\pi}{6}$	$\frac{\pi}{3}$	$\frac{\pi}{2}$
Max SAR, W/kg	0.0002911	0.095636	0.361657
θ at Max SAR, rad	0.958642	1.06644	1.57079

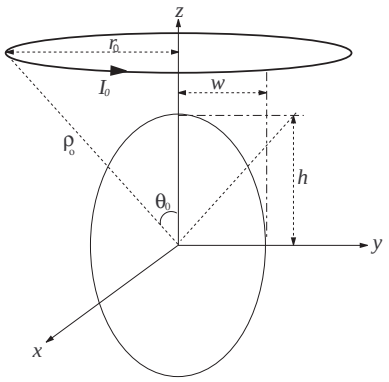

Fig. 1. Spheriod with circular wire antenna

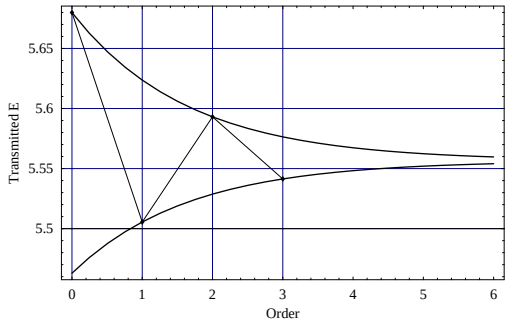

Fig. 2. Approximation of higher orders

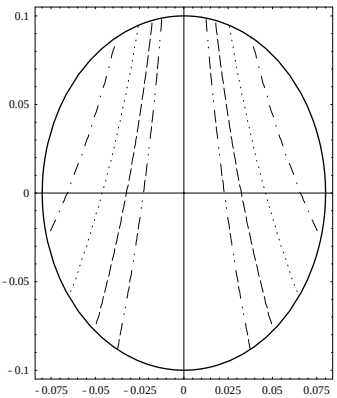

Fig. 3. SAR distributions within spheroid for $\theta_0 = 30^o$

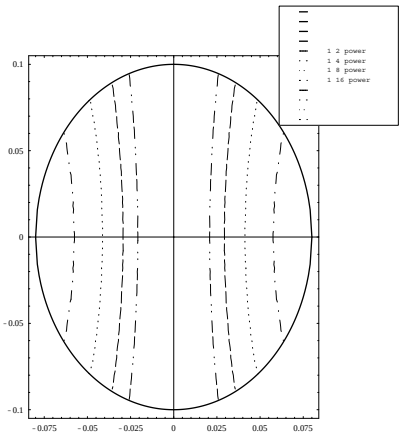

Fig. 4. SAR distributions within spheroid for $\theta_0 = 90^o$